A Full-Factors Microwave Properties Measurement System of 20m Diameter Anechoic Chamber

Wei Tian (1)(2), Yun Shao (1)(2)(3), Zhiqu Liu (2), Qiufang Wei(1)(3), Zhihua Tang(4), Chong Ni(4)

[1] Aerospace Information Research Institute, Chinese Academey of Sciences, 20(A) Datun Road, Chaoyang District, Beijing, 100101, China

[2] Laboratory of Target Microwave Properties (LAMP), Deqing, Zhejiang, 313200, China

[3] University of Chinese Academy of Sciences, 19(A) Yuquan Road, Shijingshan District, Beijing, 100049, China

[4] Institute of Remote Sensing Satellite, China Academy of Space Technology, 104 Youyi Road, Haidian District, Beijing, 100094, China

Email: tianwei@aircas.ac.cn; shaoyun@aircas.ac.cn; lzq@dasa.net.cn; weiqf@aircas.ac.cn

Abstract: Measurement of microwave characteristics for targets in an anechoic chamber could improve the cognition of EM waves scattering mechanism. In this paper, a Full-Factors Microwave Properties Measurement System (FFMPMS) was introduced, including the overall capabilities, the mechanical structures, the antenna RF system and etc. The Radar Cross Section (RCS) measurement and SAR images measured by FFMPMS, were demonstrated in this paper, when the frequencies of EM waves, the incidence angles and the azimuth angles varied. It was verified that the accuracy of RCS of a metal sphere measured by FFMPMS was 1.09dBsm and 1.00dBsm in HH and VV polarization, respectively, comparing with Mie scattering computational results, when the frequency involved ranging from 2.5GHz to 18GHz. In addition, a four-wing UAV SAR images, acquired in various azimuth direction by FFMPMS, were demonstrated.

Keywords: Microwave Properties, Measurement, RCS, SAR, Anechoic Chamber

1. INTRODUCTION

Synthetic Aperture Radar (SAR) is widely used in varied aspects such as the identification of man-made targets and the monitoring of the earthquake, flood, crops and etc.(Shao et al. 2001; Shao, Liao, and Wang 2002; Tian et al. 2015; Wang et al. 2018) In terms of application, SAR imageries are fundamentally different from optical ones, resulting in the difficulty of either interpretation or information retrieval of SAR images. In another words, SAR images are one of the projection of the natural world around us, which would outline the scenery of what you see is not what you know. SAR image consists of discrete points, lines and theirs associations, which deteriorate the unity, continuity and interpretability of SAR imageries for end users. Better understanding and cognition of SAR images could improve the utility of SAR data effectively, and optimize the algorithm that engaged in the processing of SAR data.

In recent decades, the vital problems regarding radar remote sensing are as follows.

(1)The lack of a platform for measuring the microwave characteristics of ground objects in a strictly controllable environment and thus the lack of the fundamental scientific data accumulated. (2) Many of the existing theoretical models of microwave remote sensing are based on some assumptions, and many hypotheses cannot be verified. (3) Many of the existing models, in the field of radar remote sensing application, are based on statistical models, physical models are expected though. All of above factors limit the wide application of radar remote sensing data, especially the original innovation.

Some microwave measurement laboratories have been built worldwide in decades. But most of them are engaged in hardware system research, defense study, or technology applications. Such as the electromagnetic and microwave Laboratory (EML) of Texas A & M University and the information and communication technology center (ICT) of Commonwealth Scientific and Industrial Research Organization (CSIRO), Antenna and Scattering Laboratory (ASL), National University of Singapore (ASL), Computational Electromagnetics Laboratory (CEL), Department of Aviation Systems, National Aeronautics and Astronautics Laboratory of India(Jung et al. 2015). In addition, some laboratories have carried out the measurement and Application Research of microwave remote sensing basic theory, such as the European Microwave Signature Laboratory (EMSL)(Mattia et al. 1995) and the Radiation Laboratory of the Department of Electrical Engineering and Computer Science of the University of Michigan, Radlab). All of above laboratories have carried out a large number of indoor and outdoor scattering measurement experiments, accumulated a certain number of typical ground object scattering characteristics data, and developed professional scattering models regarding radar remote sensing technology(Brunner et al. 2007; Cloude and Papathanassiou 1997; Mancini et al. 1995).

In this paper, the Full-Factors Microwave Properties Measurement System (FFMPMS) was introduced, and some of the measurement and imagines acquired by the system were demonstrated.

2. THE FFMPMS

2.1 Overall Capabilities

The Full-Factors Microwave Properties Measurement System (FFMPMS), operating in the 20m diameter anechoic chamber that shields any EM outside, could carry out the so called full factors continuous microwave spectrum measurement for the investigated targets, with azimuth angle of 0-360 °, incident angle of 0-180 °, full polarization mode, frequency of 0.8GHz-20GHz. The internal size of FFMPMS is: 24m (length) × 24m (width) × 17m (height), as shown in Fig. 1-Fig.2. The positioning accuracy of the straight orbit system of FFMPMS is 0.1 mm, while 0.01 ° for the arc orbit. This guarantees that FFMPMS could implement the quantitative control of the relative motion between the antenna and the target under measurement, with high-precision. The dynamic range of FFMPMS is better than 100 dB, and the sensitivity is greater than - 60 dBsm. The platform could conduct eighter imaging in conventional SAR imaging modes such as spotlight, stripmap and ISAR or in

complex SAR imaging modes such as POLSAR, InSAR, polInSAR, with the highest spatial resolution is as high as 1cm.

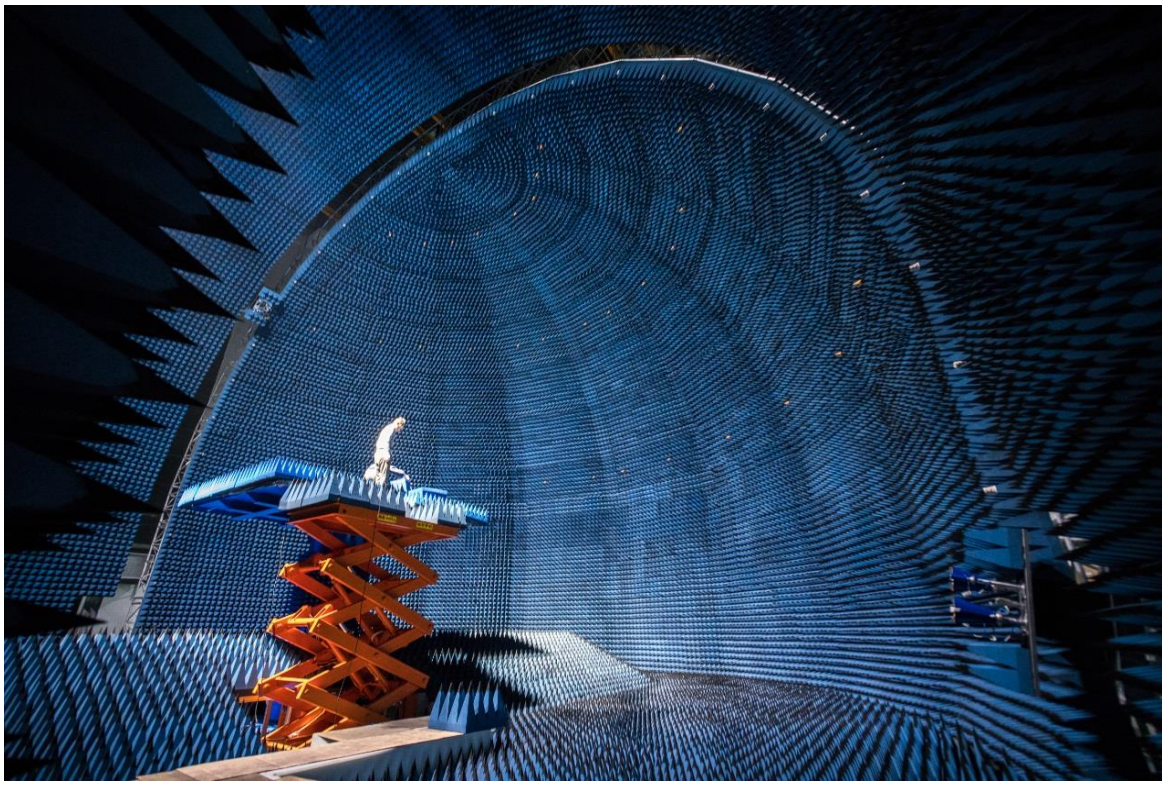

Fig.1 The inner view of FFMPMS.

Fig.2 The front view of FFMPMS.

2.2 Mechanical Structures

The dome of FFMPMS is built with aluminum racks, where an accurate arc orbit is installed in it, as shown in Fig. 3. The two sets of antenna, sliding along with the arc orbit where the

antennas themself are mounted on, are driven by the two long and curve arms that are installed above the top of the dome. The precise curve orbit is critical to guarantee the positioning precision of moving antenna.

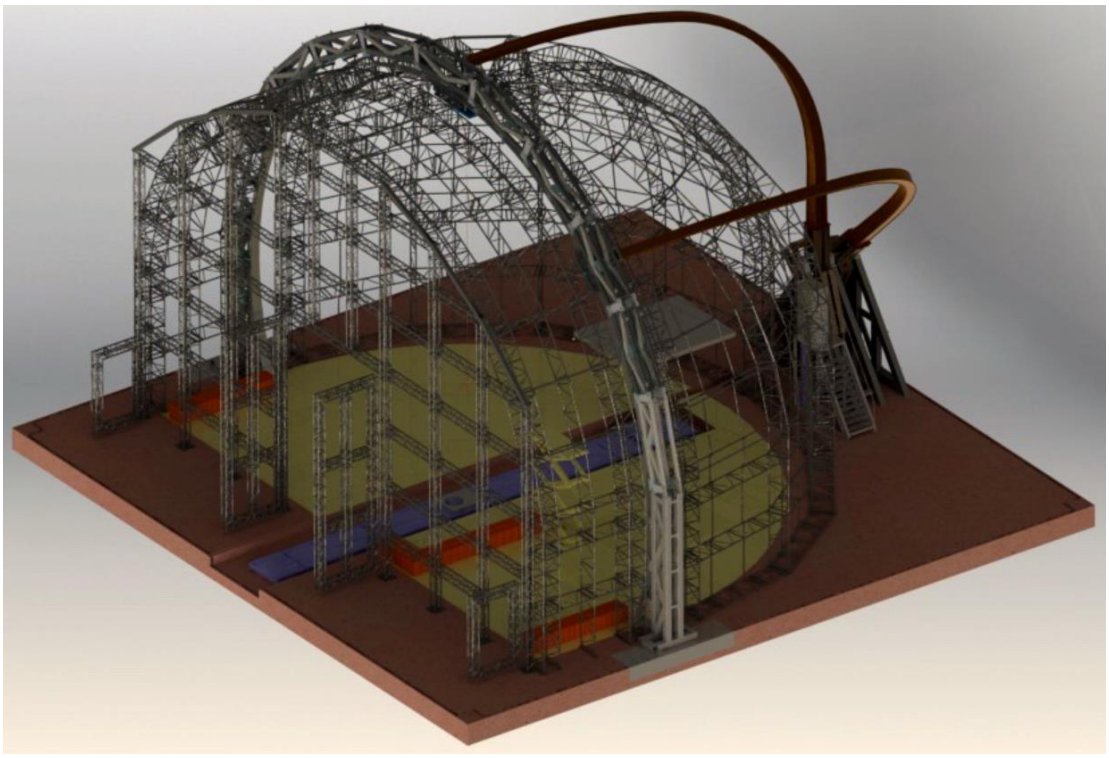

Fig. 3 The illustrated map of the structure of FFMPMS dome.

2.3 Antenna RF System

There are two sets of antenna in FFMPMS: lower band (0.8GHz-6GHz) antennas (QR-800, total two) and higher band (6GHz-18GHz) antenna (QR-6000, total two), as shown in the Tab. 1. Each of the antenna pair is divided to transmit one (Tx) and receive one (Rx). The signal, input to the Tx channel, is coming from the Vector Net Analyzer (VNA, N5222A of Keysight, USA) of the platform. The signal, received by the Rx antenna, on the other hand, is output to the Rx channel of the system and is processed by VNA as well. See Fig. 4 as reference.

Tab. 1 The comparison between the two types of antenna.

Specificaitons	**QR800**	**QR6000**
Frequency range	0.8GHz-6GHz	6GHz-18GHz
Average gain	7–18 dBi	10–18 dBi
Average VSWR	<1.9:1	<1.9:1
Return loss	<-10 dB	<-10 dB
Polarization	Dual linear	Dual linear
Cross-pol discrimination	>30 dB	>30 dB
Port-to-port isolation	>30 dB	>35 dB
Impedance	50 Ohms	50 Ohms

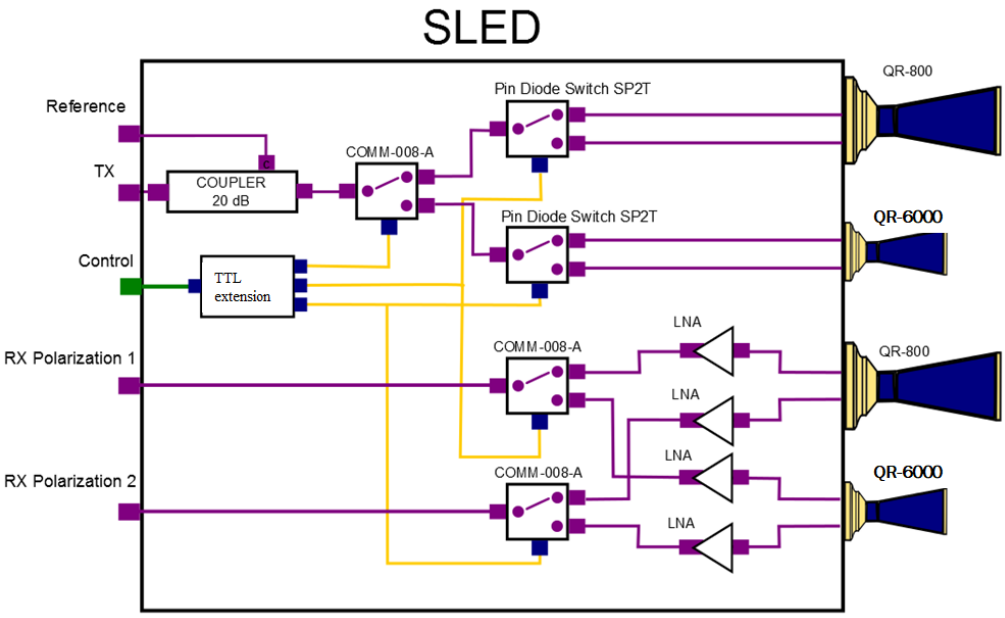

Fig. 4 The diagram of antenna RF system of FFMPMS.

3. SCATTERING AND IMAGING EXPERIMENTS

3.1 Calibration

A three-target polarization calibration algorithm for microwave anechoic chamber is used in FFMPMS(Wiesbeck and Kahny 1991). The algorithm calibrates 12 error coefficients of the repolarization scattering matrix by three kinds of reference targets, including four isolation error coefficients, four transmitting error coefficients and four receiving error coefficients.

3.2 Scattering Measurement of A Medal Sphere

A medal sphere with radius of 32cm was measured under incidence of 45°, azimuth angle of 0°, and frequency band of 1-18GHz. Further, the computational solution of RCS in terms of Mie theory(Xu 2017) was proposed for comparison, see Fig.5-Fig.6.

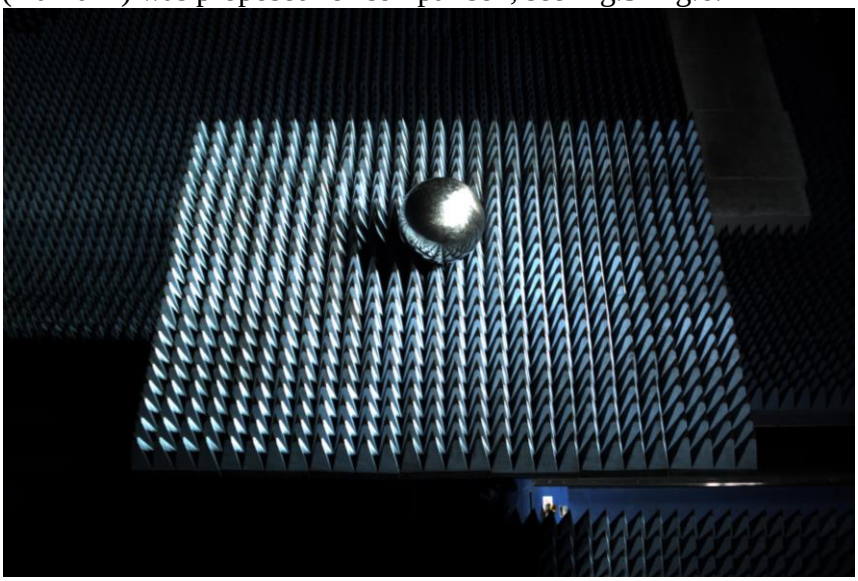

Fig. 5 The medal sphere is under measurement in FFMPMS.

In Fig.6, we are able to summarize the following conclusion. In the range of 2.5 ~ 18GHz,

the root mean square error of RCS between the measured values and Mie series solution is 1.09dBsm and 1.00dBsm at HH and VV polarization, respectively. Moreover, it can be observed that the deviation from Mie series solution is worse than 1dBsm when the frequency applied is either lower than 2.5GHz or higher than 17GHz. The possible reason is that the surface of the tested metal ball is not smooth enough, comparing with the ideal one. In the range of 1-2.5GHz, some of the measured values fluctuate greatly. This is because, on the one hand, the calibration accuracy of FFMPMS in the low-frequency region is not as good as expected. On the other hand, the lower frequency band is located in the EM resonance region, in terms of the radius of the metal ball, which is equivalent to the radar wavelength.

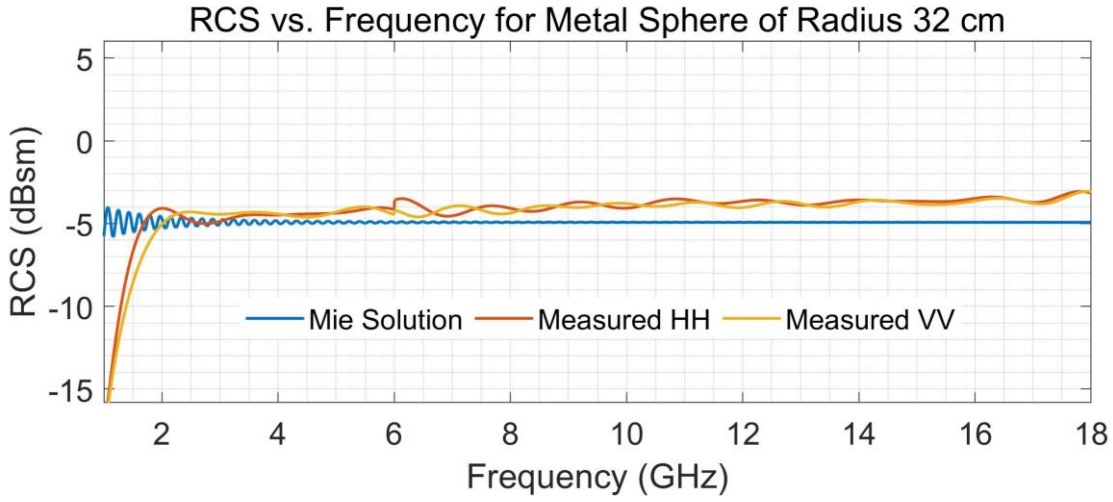

Fig. 6 The RCS measured by FFMPMS VS. Mie solution for a medal sphere (Φ=32cm).

3.3 Imaging Experiment of A UAV

The BP (back projection) imaging algorithm was applied in FFMPMS. The principle of BP is to determine a target function by calculating the position of the measured target at different azimuth times and coherently stacking the echo signals at each azimuth time(Santosa and Vogelius 1990; Yegulalp 1999). A sample of imaging for UAV (Fig. 7) was introduced in this paper, see Tab. 2 for references.

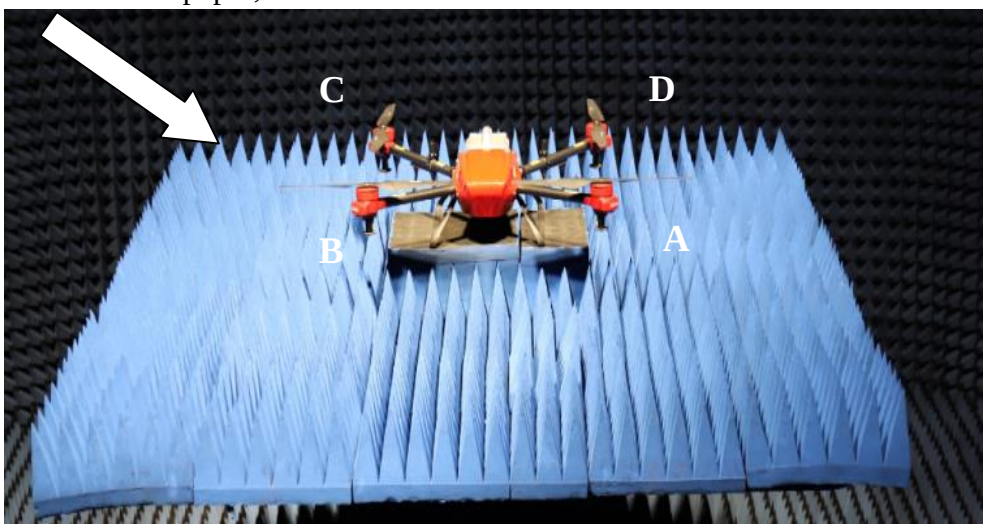

Fig. 7 The four-wing UAV is under measurement in FFMPMS (The arrow indicates the direction of the incidence EM waves).

Fig. 8 shows images of the UAV in various directions relative to the incidence EM waves, which are implemented by FFMPMS. We can see that the characteristics of both the wings

and reflecting corners of UAV varied when the azimuth angle changed. One can deduce the orientation of UAV by discriminating the discrete structure from the images. In general, it is expected that the wings of UAV whose long axis is perpendicular to the incidence EM waves are subject to be detected by radar. In this case, for example, wing A and wing C, including the connecter between the wing and the body of UAV, were full images by the antenna in the direction of 225 °.

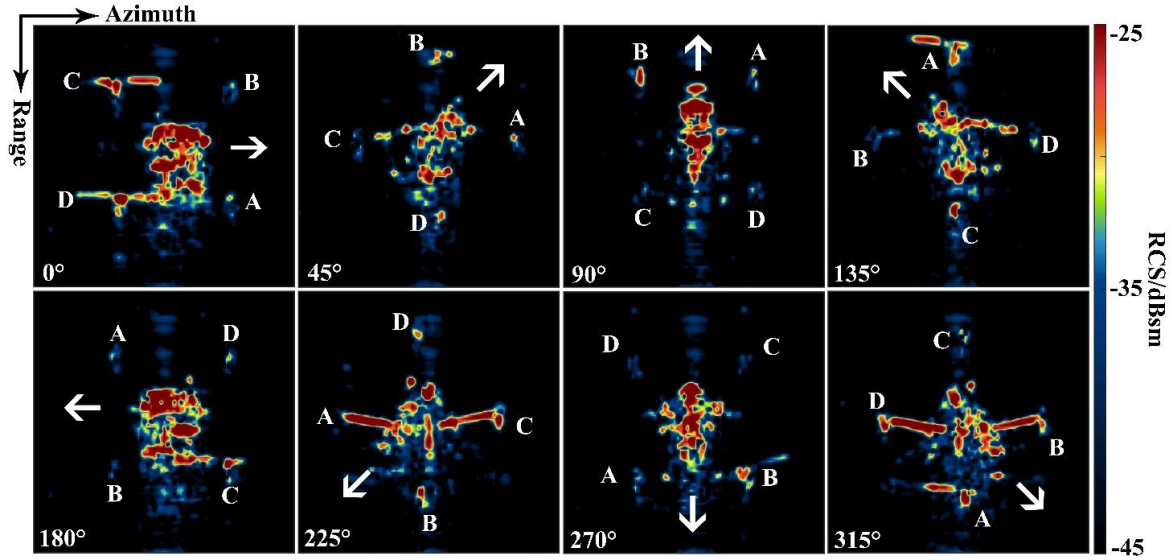

Fig. 8 The ISAR images of the four-wing UAV by FFMPMS (In Ku band, the arrow indicates the direction of the head of UAV).

Tab. 2 Imaging parameters for UAV.

Incidence angle (°)	**25**	**35**	**45**	**55**
Extent of rotation (°)	24	24	28	28
Central frequency (GHz)	15	15	15	15
Band width (GHz)	6.0	6.0	6.0	6.0
Resolution in range direction (m)	0.06	0.04	0.04	0.03
Resolution in azimuth direction (m)	0.06	0.04	0.03	0.03

4. CONCLUSIONS

The scattering and imaging capability of FFMPMS were demonstrated in this paper, considering multi-measurement mode, multi-frequency band, multi-incidence and multi-azimuth angle. The experiment results of the medal ball show that the scattering measurement results are in good agreement with the theoretical values in FFMPMS, especially when the frequency band applied is higher than 2.5GHz. The multi azimuth angle imaging experiment of four-wing UAV shows that the target with complex structure can be imaged by multi angle SAR. One can expect to detect target with complicate components by interpreting the SAR image in various azimuth direction.

References

Brunner, Dominik, Guido Lemoine, Joaquim Fortuny, and Lorenzo Bruzzone. 2007. "Building Characterisation in VHR SAR Data Acquired under Controlled EMSL Conditions." Pp. 2694–97 in *2007 IEEE International Geoscience and Remote Sensing Symposium*. Vol. 33. IEEE.

Cloude, S. R., and K. P. Papathanassiou. 1997. "Polarimetric Optimisation in Radar Interferometry." *Electronics Letters* 33(13):1176.

Jung, Richard, Winny Adolph, Manfred Ehlers, and Hubert Farke. 2015. "A Multi-Sensor Approach for Detecting the Different Land Covers of Tidal Flats in the German Wadden Sea - A Case Study at Norderney." *Remote Sensing of Environment* 170(12):188–202.

Mancini, M., F. Vandersteene, P. A. Troch, O. Bolognani, G. Terzaghi, G. D'Urso, and M. Wuthrich. 1995. "Experimental Setup at the EMSL for the Retrieval of Soil Moisture Profiles Using Multifrequency Polarimetric Data." Pp. 2023–25 in *1995 International Geoscience and Remote Sensing Symposium, IGARSS '95. Quantitative Remote Sensing for Science and Applications*. Vol. 3. IEEE.

Mattia, F., J. Fortuny, G. Nesti, and A. J. Sieber. 1995. "Quality Analysis of Strip Map SAR Products Obtained at EMSL." Pp. 171–75 in *Proceedings International Radar Conference*. IEEE.

Santosa, Fadil, and Michael Vogelius. 1990. "A Backprojection Algorithm for Electrical Impedance Imaging." *SIAM Journal on Applied Mathematics* 50(1):216–43.

Shao, Yun, Xiangtao Fan, Hao Liu, Jianhua Xiao, S. Ross, B. Brisco, R. Brown, and G. Staples. 2001. "Rice Monitoring and Production Estimation Using Multitemporal RADARSAT." *Remote Sensing of Environment* 76(3):310–25.

Shao, Yun, Jingjuan Liao, and Cuizhen Wang. 2002. "Analysis of Temporal Radar Backscatter of Rice: A Comparison of SAR Observations with Modeling Results." *Canadian Journal of Remote Sensing* 28(2):128–38.

Tian, W., X. Bian, Y. Shao, and Z. Zhang. 2015. "On the Detection of Oil Spill with China's HJ-1C SAR Image." *Aquatic Procedia* 3:144–50.

Wang, Xiaochen, Yun Shao, Wei Tian, and Xiaolin Bian. 2018. "An Investigation into the Capability of Compact Polarized SAR to Classify Multi-Sea-Surface Characteristics." *Canadian Journal of Remote Sensing* 44(2):91–103.

Wiesbeck, W., and D. Kahny. 1991. "Single Reference, Three Target Calibration and Error Correction for Monostatic, Polarimetric Free Space Measurements." Pp. 1551–58 in *Proceedings of the IEEE*. Vol. 79.

Xu, Xiaojian. 2017. *New Techniques for Radar Target Scattering Signature Measurement and Processing*. 1st ed. Beijing, China: National Defense Industry Press of China.

Yegulalp, A. F. 1999. "Fast Backprojection Algorithm for Synthetic Aperture Radar." Pp. 60–65 in *Proceedings of the 1999 IEEE Radar Conference. Radar into the Next Millennium (Cat. No.99CH36249)*. IEEE.